

Furutsu-Novikov-like cross-correlation-response relations for systems driven by shot noise

Jakob Stubenrauch^{1,2,*} and Benjamin Lindner^{1,2}

¹*Bernstein Center for Computational Neuroscience Berlin, Philippstraße 13, Haus 2, 10115 Berlin, Germany*

²*Physics Department of Humboldt University Berlin, Newtonstraße 15, 12489 Berlin, Germany*
(Dated: September 30, 2024)

We consider a dynamic system that is driven by an intensity-modulated Poisson process with intensity $\Lambda(t) = \lambda(t) + \varepsilon\nu(t)$. We derive an exact relation between the input-output cross-correlation in the spontaneous state ($\varepsilon = 0$) and the linear response to the modulation ($\varepsilon > 0$). If ε is sufficiently small, linear response theory captures the full response. The relation can be regarded as a variant of the Furutsu-Novikov theorem for the case of shot noise. As we show, the relation is still valid in the presence of additional independent noise. Furthermore, we derive an extension to Cox-process input, which provides an instance of colored shot noise. We discuss applications to particle detection and to neuroscience. Using the new relation, we obtain a fluctuation-response-relation for a leaky integrate-and-fire neuron. We also show how the new relation can be used in a remote control problem in a recurrent neural network. The relations are numerically tested for both stationary and non-stationary dynamics. Lastly, extensions to marked Poisson processes and to higher-order statistics are presented.

I. INTRODUCTION

Numerous systems in nature generate random sequences of events, which in turn drive other systems. For instance, the photocurrent in a detector [1], the spontaneous vacuum current in an electrode [2], neural firing driven by other neurons' spikes [3], and an economy subject to the effect of seismic events [4] are all examples for systems driven by random point processes.

A first approach to quantify the relation of a driving process and an observable of the system is to compute the cross-correlation function. Cross-correlations quantify the similarity of fluctuations in the drive and the observable, yet they cannot be straightforwardly used to predict the response to systematic perturbations of the drive. The latter can be quantified by linear-response functions.

If the driving process is colored Gaussian noise, the two important statistics, cross-correlation functions and linear-response functions, are linearly related by the Furutsu-Novikov theorem (FNT) [5, 6], also known as Gaussian integration by parts [7]. The relation has been frequently applied to study wave propagation in random media [8], turbulent flow [7, 9, 10], neural systems [11–13], and general stochastic processes [14–17]. In the neural context, the FNT is particularly interesting: In the absence of an external stimulus, neurons in the cortex are not silent but spike spontaneously [18, 19]; when a weak stimulus is applied, the neurons respond linearly [19–23]. As one of us showed [11] using the FNT, spontaneous fluctuations and linear response can be connected in a fluctuation-response relation (FRR). Yet, since the FNT relies on Gaussian noise, shot-noise-driven systems, such

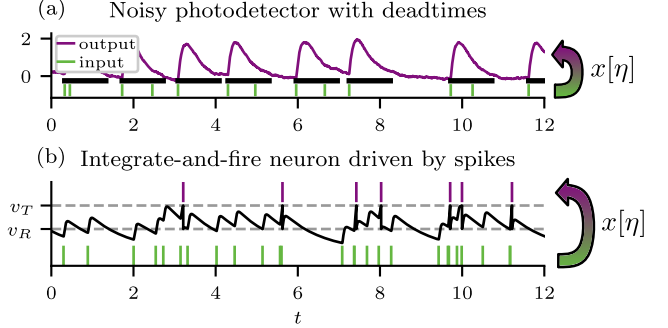


Figure 1. Examples of trajectories of shot-noise-driven systems. (a) Output (purple line) of a nonparalyzable photodetector with deadtimes (black bars) driven by shot noise (green lines). (b) Voltage trace (black), output spikes (purple), and input spikes (green) for a leaky integrate-and-fire neuron Eq. (32).

as the systems mentioned above are not captured by this approach.

Modeling shot noise as Gaussian noise, known as the diffusion approximation [3], is only justified due to the central limit theorem if the intensity of events is high and their amplitude is low. However, for pyramidal neurons, as few as two input spikes can be sufficient to trigger an output spike [24, 25], which renders results based on the diffusion approximation inaccurate [26]. Also for the broad problem of particle detection, the shot-noise character of the input cannot be neglected in many cases of interest. To extend the theory of stochastic processes from a Gaussian description to a true shot-noise description, an important stepping stone is to find an analogue of the FNT for shot-noise-driven systems. Such an analogue must attribute input-output cross-correlations of a shot-noise-driven black box to the response functions of

* Corresponding author. jakob.stubenrauch@rwth-aachen.de

the black box.

In this paper we first consider an arbitrary system driven by an inhomogeneous Poisson process, and derive a relation between its spontaneous input-output cross-correlation and its response to a time-dependent modulation of the input intensity. This cross-correlation–response relation (CRR) can be regarded as a shot-noise analogue of the original FNT. Although all necessary tools to do so are known [27], such a relation has to our knowledge not been reported yet. We then discuss the impact of additional noise and derive an extension to the case where the input is correlated shot noise. Next, we test the CRR for a minimal model of a particle detector and for a leaky integrate-and-fire neuron. For the leaky integrate-and-fire neuron, we leverage the CRR and the method of [11] to derive an FRR between the spontaneous *output* fluctuations of a shot-noise-driven neuron and its systematic response to a time-dependent intensity modulation. We numerically test the CRR and the FRR in the commonly studied stationary case but demonstrate that the validity of the CRR extends to a non-stationary scenario. Furthermore, we show how the CRR can be applied to the problem of remote control in a recurrent neural network. Lastly, we present extensions to Poissonian input with random amplitudes and to nonlinear response functions.

II. CROSS-CORRELATION–RESPONSE RELATION

We denote a system’s observable $x[\eta(\circ); t]$ by a functional of the entire input process $\eta(\circ)$. Both, the intrinsic time argument \circ and the functional dependence on η , will be hidden, whenever not explicitly required, to ease the notation. The additional scalar dependence on the observation time t must reflect causality. A simple example is linearly filtered shot noise, $x_\kappa(t) = \int^t dt' \kappa(t-t')\eta(t')$; however, the following applies to general functionals.

We consider inhomogeneous Poissonian input

$$\eta(t) = \sum_i \delta(t - t_i), \quad (1)$$

where t_i are Poisson events with intensity $\Lambda(t) = \lambda(t) + \varepsilon\nu(t)$, $\lambda(t)$ is the baseline, and $\varepsilon\nu(t)$ is a modulation. We denote the observable’s average over spontaneous ($\varepsilon = 0$) realizations of the input by $\langle x(t) \rangle_0$, thus the cross-correlation function between the input events and the output without modulation is

$$C_{x\eta}(t, t') = \langle x(t)\eta(t') \rangle_0 - \langle x(t) \rangle_0 \langle \eta(t') \rangle_0. \quad (2)$$

If we switch on the modulation, the average effect on the observable can be represented perturbatively by a linear-response function K ,

$$\langle x(t) \rangle_\varepsilon = \langle x(t) \rangle_0 + \varepsilon \int dt' K(t, t')\nu(t') + \mathcal{O}(\varepsilon^2). \quad (3)$$

The $\mathcal{O}(\varepsilon^2)$ corrections can be omitted for a sufficiently weak modulation, and the linear-response function is given by a functional derivative [28]

$$K(t, t') = \left. \frac{\delta}{\delta\Lambda(t')} \langle x(t) \rangle_0 \right|_{\Lambda=\lambda}, \quad (4)$$

where

$$\frac{\delta}{\delta f(t)} g[f] \equiv \left. \frac{d}{dh} g[f(\circ) + h\delta(t - \circ)] \right|_{h=0} \quad (5)$$

captures the infinitesimal change of a functional due to an infinitesimal perturbation at time t .

In the following, we express both the response- and the cross-correlation functions by the characteristic functional of the input process which leads us to the CRR. Specifically, we represent $x[\eta; t]$ by its functional Fourier transform with respect to η ,

$$x[\eta; t] = \int \mathcal{D}u y[u; t] e^{iu^T \eta}, \quad (6)$$

where $u^T \eta \equiv \int dt u(t)\eta(t)$ and $\int \mathcal{D}u \equiv \lim_{M \rightarrow \infty} \int_{-\infty}^{\infty} du_1 \dots \int_{-\infty}^{\infty} du_M$ with $u_i = u(t_i)$, and $\{t_1, \dots, t_M\}$ is an equidistant discretization of the interval $[0, T]$. For instance, an exponentiated linear filter $x_\beta[\eta; t] = \exp\left(\int^t dt' \beta(t-t')\eta(t')\right)$ has the functional Fourier transform $y[u; t] = \delta[iu(\circ) - \beta(t - \circ)\Theta(t - \circ)]$ with the functional Dirac delta $\delta[f(\circ)] \equiv \lim_{M \rightarrow \infty} \prod_{i=1}^M \delta(f(t_i))$ and the Heaviside function $\Theta(t)$. Thus, in general, the functional Fourier transform dissects functionals $\eta \mapsto x[\eta; t]$ into a linear combination of exponentiated linear filters. This is useful as it establishes a link to characteristic functionals, as used below. The formal limit $M \rightarrow \infty$ assumes convergence of x upon decreasing the time step T/M , which is also a requirement for Euler integration. For finite M , Eq. (6) is the usual M -dimensional Fourier transform. For a formal classification of the existence of the Fourier transform of functionals of Poisson processes, see [27, Lemma 18.4].

Plugging Eq. (6) into Eq. (4) yields

$$\begin{aligned} K(t, t') &= \int \mathcal{D}u y[u; t] \left. \frac{\delta}{\delta\Lambda(t')} \langle e^{iu^T \eta} \rangle_0 \right|_{\Lambda=\lambda} \\ &= \int \mathcal{D}u y[u; t] e^{iu(t')} Z[u] - \langle x(t) \rangle_0, \end{aligned} \quad (7)$$

where the characteristic functional of a Poisson process of intensity $\lambda(t)$ is [29]

$$Z[u] \equiv \langle e^{iu^T \eta} \rangle_0 = e^{\int \lambda(t) [e^{iu(t)} - 1] dt}. \quad (8)$$

The cross-correlation Eq. (2) can be expressed by a functional derivative of $Z[u]$ as well

$$\begin{aligned} C_{x\eta}(t, t') &= \int \mathcal{D}u y[u; t] \frac{\delta}{\delta iu(t')} Z[u] - \lambda(t') \langle x(t) \rangle_0 \\ &= \lambda(t') \left[\int \mathcal{D}u y[u; t] Z[u] e^{iu(t')} - \langle x(t) \rangle_0 \right]. \end{aligned} \quad (9)$$

Comparing this result with Eq. (7), we infer for arbitrary systems driven by Poisson noise a CRR

$$C_{x\eta}(t, t') = \lambda(t')K(t, t'). \quad (10)$$

Thus, irrespective of the details of the system, the input-output cross-correlation, a measure of the spontaneous fluctuations, can be fully attributed to the linear-response function, which determines the leading order deviations *away from* the spontaneous mean. In particular, the cross-correlation is unaffected by nonlinear response functions. Eq. (10) should be put in context with the original FNT for Gaussian noise ξ [5, 6]

$$C_{x\xi}(t, t'') = \int dt' C_\xi(t'', t') K_{x\xi}(t, t'), \quad (11)$$

where C_ξ is the noise autocorrelation function and $K_{x\xi}$ is the response of $\langle x \rangle$ to a modulation of the input mean $m(t) = \langle \xi(t) \rangle$. Remarkably, for white Gaussian noise $C_\xi(t, t') = \lambda(t')\delta(t-t')$ [recall that Poissonian noise is white, $C_\eta(t, t') = \lambda(t')\delta(t-t')$], Eq. (11) looks like Eq. (10), if we naively identify K with $K_{x\xi}$. However, there are important differences between the two response functions. $K_{x\xi}$ is the response function of the time-dependent mean output, $\langle x(t) \rangle$, with respect to a modulation of the mean input in the presence of Gaussian noise. The response function K considers the same output statistics $\langle x(t) \rangle$ but with respect to a modulation of the intensity (the rate) of the driving Poisson process, a modulation that affects not only the mean value but all higher cumulants of the driving noise and in particular the noise intensity. An additional difference is that K is also shaped by the type of background noise, which is here a Poisson process and not Gaussian noise. Hence, there are two differences and in general Eq. (10) and Eq. (11) constitute relations between input-output cross-correlations and response functions for two distinct settings (different background noise) and two different types of response functions. Nevertheless, as we show in App. B, the two relations become equivalent in a diffusion limit.

Returning to the CRR Eq. (10), for a constant baseline intensity $\lambda(t) \equiv \lambda_0$ and stationary dynamics of the driven system, we may define $C_{x\eta}(\tau) \equiv C_{x\eta}(t+\tau, t)$ and $K(\tau) \equiv K(t+\tau, t)$ such that in frequency space we have

$$S_{x\eta}(\omega) = \lambda_0 \chi(\omega), \quad (12)$$

where the cross-spectrum $S_{x\eta}(\omega) = \mathcal{F}[C_{x\eta}](\omega)$ and susceptibility $\chi(\omega) = \mathcal{F}[K](\omega)$ are the Fourier transforms $\mathcal{F}[f](\omega) = \int dt e^{i\omega t} f(t)$ of $C_{x\eta}$ and K respectively.

For the linearly filtered shot noise x_κ introduced above, Eq. (10) can be checked directly: Using the statistics of Poisson processes [29] one gets $C_{x_\kappa\eta}(t, t') = \lambda(t')\kappa(t-t')\Theta(t-t')$ and $K(t, t') = \kappa(t-t')\Theta(t-t')$, which confirms the CRR. In Sec. III, we demonstrate the validity of Eq. (10) for systems for which the explicit computation of the statistics of interest is not feasible. Next, we present two useful extensions of the CRR.

A. Extension: additional noise

Here we consider the prevalent situation in which the shot-noise-driven system receives additional noise, for instance thermal noise or the input of other random forces. The system's output at observation time t may be an arbitrary functional $\hat{x}[\eta, \xi; t]$ of both, the Poissonian input η and the additional random force ξ . Assuming statistical independence of η and ξ , the ξ -averaged cross-correlation between the Poissonian drive η and the output \hat{x} is

$$\begin{aligned} \langle C_{\hat{x}\eta}(t, t') \rangle_\xi &\equiv \langle \langle \hat{x}[\eta, \xi; t] \eta(t') \rangle_\eta - \langle \hat{x}[\eta, \xi; t] \rangle_\eta \langle \eta(t') \rangle_\eta \rangle_\xi \\ &= \langle \langle \hat{x}[\eta, \xi; t] \rangle_\xi \eta(t') \rangle_\eta - \langle \langle \hat{x}[\eta, \xi; t] \rangle_\xi \rangle_\eta \langle \eta(t') \rangle_\eta \\ &\equiv C_{\langle \hat{x} \rangle_\xi \eta}(t, t'). \end{aligned} \quad (13)$$

This is equal to the cross-correlation between the Poissonian drive η and the ξ -averaged output $\langle \hat{x} \rangle_\xi$. Furthermore, we may interchange the order of ξ -averaging and applying a linear differential operator, thus the ξ -averaged response of \hat{x} to modulations of the intensity of η is

$$\left\langle \frac{\delta}{\delta\Lambda(t')} \langle \hat{x}(t) \rangle_\eta \right\rangle_{\Lambda=\lambda} \Big|_\xi = \frac{\delta}{\delta\Lambda(t')} \langle \langle \hat{x}(t) \rangle_\xi \rangle_\eta \Big|_{\Lambda=\lambda}. \quad (14)$$

When defining $x[\eta; t] \equiv \langle \hat{x}[\eta, \xi; t] \rangle_\xi$, we are back at the case without additional noise discussed above. Thus, for additional noise sources that are independent of the drive η , the CRR Eq. (10) is still valid. For an experimenter this means that, for instance, uncontrolled thermal fluctuations are not detrimental for the CRR and will simply average out. This fact is exploited in Sec. III A.

B. Extension: shot noise with temporal correlations

The Poisson process considered so far is white noise $C_\eta(t, t') \propto \delta(t-t')$, and we assumed knowledge of $\lambda(t)$. Both assumptions can for instance be problematic when studying neural networks. A useful noise model solving both problems is the Cox process, or doubly stochastic Poisson process, where events are conditionally Poissonian with intensity $\lambda(t)$, but $\lambda(t)$ is itself a random process. Here, we choose the intensity $\lambda(t) = \Theta[\phi(t)]\phi(t)$ where $\phi(t)$ is a Gaussian process and we assume that the mean $m(t)$ and autocorrelation $C_\phi(t, t')$ are chosen such that $\phi(t) < 0$ only rarely and we may set $\lambda(t) = \phi(t)$. The limits of validity of this choice are discussed in App. C. The cumulants of the Cox process are

$$\langle \eta(t) \rangle = m(t), \quad C_\eta(t, t') = C_\phi(t, t') + m(t)\delta(t-t'), \quad (15)$$

the latter reflecting the law of total variance, thus the process is indeed temporally correlated (colored) noise. Next, we derive a somewhat involved extension of the CRR for this case. However, as we show afterwards, the involved expression can be simplified under reasonable assumptions.

1. *Exact CRR for systems driven by a Gaussian Cox process*

The characteristic functional of a Cox process with a Gaussian-process intensity is given by $Z_{m,C_\phi}[u] = \langle Z_\phi[u] \rangle_{\phi \sim \mathcal{N}(m,C_\phi)}$ [30] where $Z_\phi[u] = \exp(\int \phi(t)[e^{iu(t)} - 1] dt)$ is the characteristic functional of the Poisson process and the average is taken over the ensemble of Gaussian processes with mean m and autocorrelation C_ϕ , thus

$$Z_{m,C_\phi}[u] = e^{m^T(e^{iu}-1) + \frac{1}{2}(e^{iu}-1)^T C_\phi(e^{iu}-1)}, \quad (16)$$

where

$$\begin{aligned} f^T g &= \int dt f(t)g(t), \\ \frac{1}{2} f^T C g &= \int dt_1 dt_2 \frac{1}{2} f(t_1) C(t_1, t_2) g(t_2). \end{aligned} \quad (17)$$

To decompose the cross-correlation into linear-response functions, we need to consider the linear response

$$K_{xm}(t, t') = \frac{\delta}{\delta M(t')} \langle x(t) \rangle_{M, C_\phi} \Big|_{M=m} \quad (18)$$

to mean modulations where the subscripts of the expectation value denote the noise parameters. Additionally, we need to take into account the linear response $K_{xC_\phi}(t, t', t'')$ to autocorrelation modulations

$$C_\phi(t', t'') \rightarrow C_\phi(t', t'') + \varepsilon D_\phi(t', t''). \quad (19)$$

This response function can be defined by

$$\begin{aligned} \langle x(t) \rangle_{m, C_\phi + \varepsilon D} &= \langle x(t) \rangle_{m, C_\phi} \\ + \varepsilon \int dt' dt'' D_\phi(t', t'') K_{xC_\phi}(t, t', t'') &+ \mathcal{O}(\varepsilon^2) \end{aligned} \quad (20)$$

and $K_{xC_\phi}(t, t', t'') = \frac{\delta}{\delta C(t', t'')} \langle x(t) \rangle_{m, C} \Big|_{C=C_\phi}$ can be computed using the two-point functional derivative

$$\frac{\delta}{\delta g(t, t')} f[g] \equiv \frac{\partial}{\partial h} f[g + h\delta(\circ_1 - t)\delta(\circ_2 - t')] \Big|_{h=0} \quad (21)$$

where $\circ_{1/2}$ denote the two intrinsic time arguments of g . Proceeding analogously to the case of Poissonian input leads to a CRR for Cox-process-driven systems

$$\begin{aligned} C_{x\eta}(t, t') &= m(t') K_{xm}(t, t') \\ + \int dt'' C_\phi(t', t'') [2K_{xC_\phi}(t, t', t'') &+ K_{xm}(t, t'')] \end{aligned} \quad (22)$$

which may alternatively be written as [see Eq. (15)]

$$\begin{aligned} C_{x\eta}(t, t') &= \int dt'' [C_\phi(t', t'') 2K_{xC_\phi}(t, t', t'') \\ + C_\eta(t', t'') K_{xm}(t, t'')]. \end{aligned} \quad (23)$$

This formulation reveals a more complicated relation between the input-output cross-correlation and the response statistics than in the simpler Poissonian and

Gaussian cases, Eqs. (10) and (11), respectively, because here the right-hand side involves different statistics of the input noise as well as response functions to modulations of different parameters. Note that in the limit $C_\phi(t, t') \rightarrow 0$, in which the intensity becomes deterministic $\langle [\lambda(t) - m(t)]^2 \rangle \rightarrow 0$, Eq. (10) is recovered with $m(t) \hat{=} \lambda(t)$ and $K_{xm} \hat{=} K$. For the linear filter, Eq. (22) can be checked directly, here $K_{xC_\phi} \equiv 0$ (see App. C).

To compute the correlation response K_{xC_ϕ} numerically, one must modulate the autocorrelation function of a Gaussian process. To illustrate a way to do this, consider the Langevin equation

$$\tau_\phi \dot{\phi} = -\phi + \sqrt{2\sigma^2 \tau_\phi [1 + \varepsilon s(t)]} \xi(t), \quad (24)$$

where ξ is centered Gaussian white noise. The autocorrelation of ϕ is then for $\tau > 0$

$$\begin{aligned} C_\phi(t + \tau, t) &= \sigma^2 e^{-\tau/\tau_\phi} \\ + \varepsilon \frac{2\sigma^2}{\tau_\phi} e^{-\tau/\tau_\phi} \int_0^\infty d\Delta e^{-2\Delta/\tau_\phi} s(t - \Delta). \end{aligned} \quad (25)$$

If the spontaneous autocorrelation takes the form $\sigma^2 e^{-\tau/\tau_\phi}$, one can thus generate the modulated process by tuning s such that the second line in Eq. (25) is the desired $\varepsilon D(t + \tau, t)$, the response to which defines the function K_{xC_ϕ} . More general spontaneous situations can be achieved analogously by higher dimensional Markovian embedding.

2. *Weakly correlation-responsive regime for systems driven by a Gaussian Cox process*

For systems that respond weakly to systematic changes in the input autocorrelation (while leaving the mean input untouched), or for which the input is only weakly autocorrelated, Eq. (22) can be simplified. Specifically, when

$$\begin{aligned} \int dt'' C_\phi(t', t'') K_{xC_\phi}(t, t', t'') \\ \ll \int dt'' C_\eta(t', t'') K_{xm}(t, t''), \end{aligned} \quad (26)$$

we find the useful relation

$$C_{x\eta}(t, t') \approx \int dt'' C_\eta(t', t'') K_{xm}(t, t'') \quad (27)$$

or, for stationary processes in frequency domain,

$$S_{x\eta}(\omega) \approx S_\eta(\omega) \chi_m(\omega). \quad (28)$$

The approximate CRR for colored shot noise Eq. (27) takes the same form as the Gaussian FNT Eq. (11), but note the differences between controlling the mean of Gaussian noise and controlling the intensity of shot noise, as mentioned below Eq. (11).

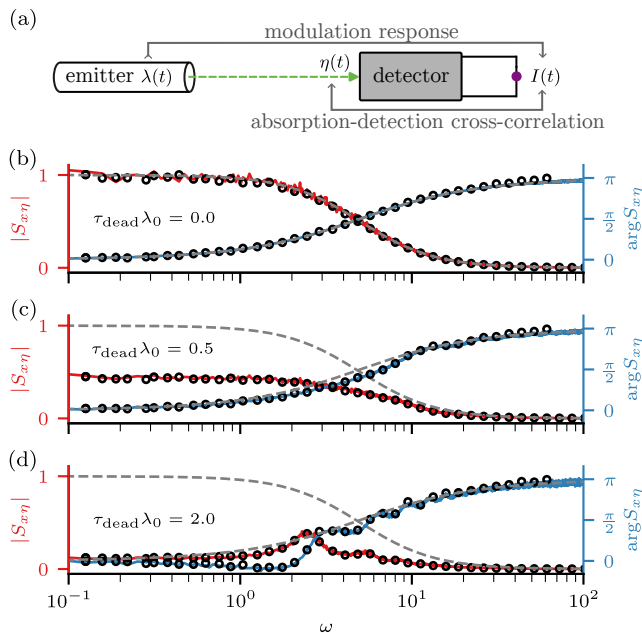


Figure 2. Test of the cross-correlation–response relation Eq. (12) for a particle detector without (b) and with deadtime (c,d) as described in Sec. III A and sketched in (a). Both, the cross-spectrum $S_{I\eta}$ (red: absolute value, blue: argument) and the susceptibility $\lambda_0\chi_{I\eta}$ (black circles) are determined from stochastic simulations (App. A) and averaged over 1000 trials – their agreement corroborates Eq. (12). (b-d) test this agreement for increasing values of the detector deadtime, making the system increasingly nonlinear, yet Eq. (12) is respected in that colored lines and black circles agree. The gray dashed lines show the exact cross-spectrum for $\tau_{\text{dead}} = 0$, that is the absolute value and argument of $\lambda_0\mathcal{F}[\alpha](\omega)$, where $\mathcal{F}[\alpha](\omega) = (1 - i\omega\tau_p)^{-2}$ is the Fourier transform of Eq. (30). Parameters: $\lambda_0 = 1$, $\tau_p = 0.2$, $\tau_\zeta = 1$, $\sigma_\zeta^2 = 0.01$, $\Delta t = 10^{-4}$, $T = 200$, $T_{\text{warm}} = 50$.

The approximation is exact for linear systems, for which always $K_{x\mathcal{C}_\phi} \equiv 0$. In Sec. III B we discuss a nonlinear system for which the approximation also holds (see Fig. 5), and in Sec. III C we show that Eq. (27) is an improvement over Eq. (10) even in a situation where the colored shot-noise input is not a Cox process.

III. APPLICATIONS OF THE CRR

A. Particle detector

Detectors resolving single particles in a beam, like electrons or photons, are of unquestionable importance: from the early Geiger Müller counters [31], used to quantify radioactive decay, to the newest superconducting-nanowire single-photon-detectors [32], key elements for optical quantum computing, to name only two prominent examples. These single particle detectors have the following issues in common [33, 34]: (i) after detecting one

particle there is a non-vanishing deadtime within which subsequent particle detection is unreliable and (ii) they are subject to thermal noise, which is problematic at the low energies corresponding to single particles. Here, we consider a generic detector model describing an observable current

$$I(t) = [\alpha * (\vartheta[\eta]\eta)](t) + \zeta(t) \quad (29)$$

which generates a pulse

$$\alpha(t - t_i) = \Theta(t - t_i) \frac{t - t_i}{\tau_p^2} \exp\left[-\frac{t - t_i}{\tau_p}\right] \quad (30)$$

upon particle arrival at t_i , provided the detector is not in a refractory state (dead) due to a preceding event. Specifically, we consider a nonparalyzable detector [31], which means that the switch ϑ attains the values $\vartheta[\eta; t] = 0$ if $\int_{t-\tau_{\text{dead}}}^t \vartheta[\eta; t']\eta(t')dt' = 1$ and $\vartheta[\eta; t] = 1$ else. The initial value of the switch, e.g. $\vartheta[\eta; 0] = 1$ corresponding to an initially susceptible detector, is forgotten after $\approx \tau_{\text{dead}}(\tau_{\text{dead}}\lambda_0)(1 + \tau_{\text{dead}}\lambda_0)$. We also take into account thermal fluctuations in the form of an Ornstein-Uhlenbeck process

$$\tau_\zeta \dot{\zeta} = -\zeta + \sqrt{2\sigma_\zeta^2\tau_\zeta}\xi(t) \quad (31)$$

[here, $\xi(t)$ is standard Gaussian white noise].

Particle emission is often considered a Poisson process, matching the key assumption in the derivation of the CRR. For instance, in the case of coherent laser light, the photon absorption statistics is exactly Poissonian [35]. Thus we may use Eq. (12) to relate the cross-spectrum $S_{I\eta}$ between the incoming particles and the elicited current to the susceptibility $\chi_{I\eta}$ with respect to modulating the beam intensity $\lambda_0 + \varepsilon\nu(t)$, namely $S_{I\eta} = \lambda_0\chi_{I\eta}$. We note that the independent thermal noise $\zeta(t)$ does not affect the relation according to what we discussed in Sec. II A.

In Fig. 2 we show the left- and right-hand sides of Eq. (12) for three different values of the detector's deadtime, where the statistics are measured in stochastic simulations, on which we elaborate in App. A. For $\tau_{\text{dead}} = 0$, we have the simple example of linearly low-pass filtered shot noise, for which both, the input-output cross-spectrum and the susceptibility drop monotonically with frequency. The system becomes nonlinear for nonvanishing deadtimes. As we see in Fig. 2(c) and (d) the detector is less susceptible in this regime, i.e. we observe an overall reduction of both the susceptibility and the cross-spectrum and for long deadtimes [Fig. 2(d)], we even see maxima forming in the spectral measures. In all cases, the CRR is excellently confirmed by the simulation results. As sketched in Fig. 2(a), in an experiment, the accessible manipulation of the beam intensity and the observable mean response to it thus permit to determine the exact cross-correlation between the actual particle arrivals and the detector signal.

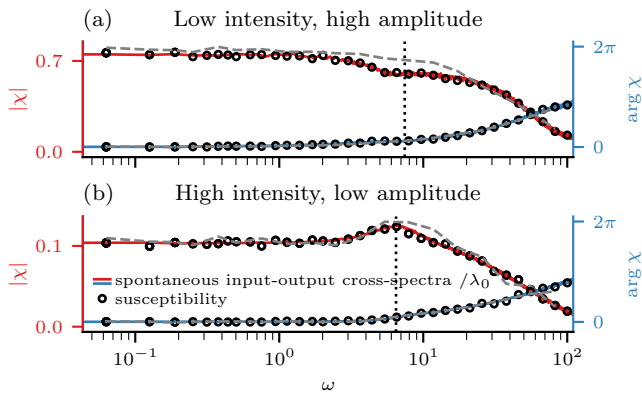


Figure 3. LIF neuron model: Test of the cross-correlation–response relation Eq. (12) for a constant baseline intensity λ_0 and the two cases of low intensity λ_0 and high amplitude A (a) and high intensity and low amplitude (b). Both, the spontaneous input-output cross-spectra $S_{x\eta}/\lambda_0$ (red lines: absolute value, blue lines and right axis: argument), and the susceptibility $\chi(\omega)$ (black circles, absolute value and argument respectively) are determined from numerical simulations (App. A); for the susceptibility the intensity is explicitly modulated ($\varepsilon > 0$). The agreement of colored lines and black circles corroborates Eq. (12). Susceptibility based on the diffusion approximation Eq. (34) (gray dashed line). Output firing rate (black dotted vertical lines). Eq. (32) is integrated by Euler’s method with time step $\Delta t = 10^{-4}$ and integration length $T = 100$. Furthermore, $v_T = 1$, $v_R = 0.5$, $\mu = 0.5$, and $\tau_s = 0.02$. In (a), $\lambda_0 = 2$, $A = 0.4$, in (b) $\lambda_0 = 16$, $A = 0.05$. The stimulus used to compute the susceptibility (circles) is $\varepsilon \cos(\omega_s t)$ with $\varepsilon = 0.1$ (a) and $\varepsilon = 0.16$ (b).

B. Leaky integrate-and-fire neuron

Integrate-and-fire neurons are an abstraction of neural dynamics that is excellent at predicting neural spike trains [25, 36–39] and frequently used in simulations and in theory of spiking neural networks [40–46]. Such models exhibit a multitude of biologically observed network states (see [41, 43] and references therein).

Here, we consider a leaky integrate-and-fire (LIF) neuron. In this model, the neuron maps the Poissonian input spikes $\eta(t) = \sum_i \delta(t - t_i)$ to its output by integrating the equation

$$\tau_m \dot{v}(t) = -v(t) + \mu + (\alpha * \eta)(t) \quad (32)$$

until the membrane voltage $v(t)$ hits a threshold $v(t_i^{\text{IF}}) = v_T$ at which the neuron spikes and is reset $v(t_i^{\text{IF}}) \rightarrow v_R$, see Fig. 1(b). Time is counted in multiples of the membrane time constant τ_m , which to ease the notation, we set to one. The neuron receives a constant current μ , and the input spikes are convolved with a synaptic filter $\alpha(t) = A \Theta(t) t \exp(-t/\tau_s)/\tau_s^2$, where A is the synaptic amplitude and $\tau_s \ll 1$ is the synaptic timescale. The output spike train $x[\eta; t] = \sum_i \delta(t - t_i^{\text{IF}})$, where t_i^{IF} are the fire-and-reset times, is communicated to other neurons and is thus the observable we are interested in.

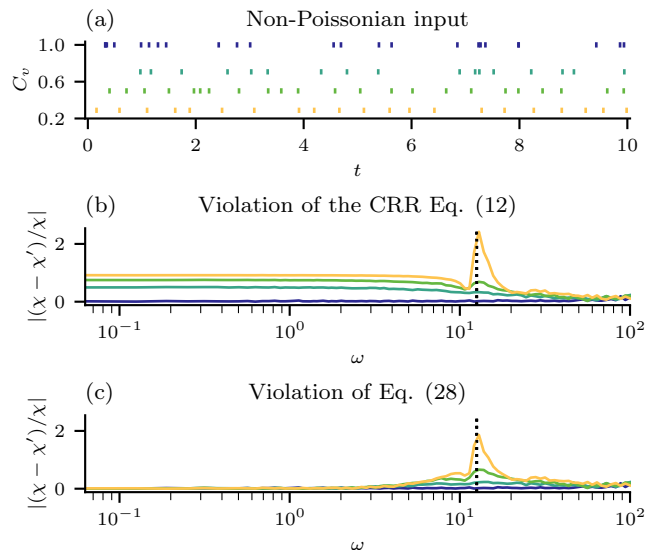


Figure 4. LIF neuron model: Violation of the CRR Eq. (12) for non-Poissonian input. (a) Samples of a Poissonian process (dark blue) and non-Poissonian processes ($C_v < 1$). (b) Absolute value of the relative error of Eq. (10) $|\chi(\omega) - S_{x\eta}(\omega)/\lambda_0|/|\chi(\omega)|$ where $\chi(\omega)$ is the response to a modulation and $S_{x\eta}(\omega)/\lambda_0$ is the spontaneous cross-spectrum. As in Fig. 3, both the susceptibility χ and the input-output cross-spectrum $S_{x\eta}$ are obtained from numerical simulations, see App. A. For all but the lowest line, the input is non-Poisson with colors corresponding to (a). The dotted line indicates the input intensity $2\pi\lambda_0$. (c) Absolute value of the error $|\chi(\omega) - S_{x\eta}(\omega)/S_\eta(\omega)|/|\chi(\omega)|$, which quantifies the mismatch of Eq. (28), for the same setting as in (b). The vanishing error at small ω indicates that here Eq. (28) is a successful color-correction of Eq. (10) whereas the remaining error about the input intensity $\omega = 2\pi\lambda_0$ indicates that here the naive color-correction fails. Parameters as in Fig. 3(a).

1. Test of the CRR and limitations for non-Poissonian input spikes

In Fig. 3 we present simulation results for the cross-spectrum $S_{x\eta}(\omega)$ using spontaneous input ($\varepsilon = 0$) and the susceptibility $\chi(\omega)$ using modulated input ($\varepsilon > 0$). Both simulations are done for two distinct parameter sets (a, b). For once, we test the case of a low input intensity with high amplitude; here two input spikes in short succession are sufficient to trigger an output spike. The susceptibility in this case is rather high and decays with increasing frequency. Secondly, we use a high input intensity with low amplitude of the input spikes (b), such that the mean input is the same as in (a) but we are close to a diffusion limit [47, 48]. In this setting we observe a much lower susceptibility (by a factor of ≈ 7 for low frequencies), which is due to the reduced synaptic amplitude A (this is similar to the findings in [26]). In addition, the high-intensity case features a peak around the firing rate that is caused by the reduction in the effective noise level. Most importantly in the context here,

in both of these opposite cases, Eq. (12) is excellently confirmed, i.e., the cross-correlation between input and output spikes in the spontaneous case fully agrees with the linear response to an intensity modulation.

A common approximation of shot-noise driven systems, the diffusion approximation [1], replaces an inhomogeneous Poisson process $\eta(t)$ with intensity $\lambda(t) + \varepsilon s(t)$ by white Gaussian noise $z(t)$ with matched first- and second-order statistics, i.e.,

$$\eta(t) \approx z(t) \equiv \lambda(t) + \varepsilon s(t) + \sqrt{\lambda(t) + \varepsilon s(t)} \xi(t), \quad (33)$$

where $\xi(t)$ is white Gaussian noise with $\langle \xi(t) \rangle = 0$ and $\langle \xi(t) \xi(t') \rangle = \delta(t - t')$. This replacement only becomes exact in a very specific scaling limit (see App. B), but is often trusted to be a good approximation. If one seeks to estimate the linear response of $\langle x[\eta; t] \rangle$ to modulations of the intensity of the Poisson process using the diffusion approximation, it becomes apparent from Eq. (33) that one has to compute the linear response of $\langle x[z; t] \rangle$ to simultaneous modulation of both, the mean and the noise intensity of the Gaussian process $z(t)$. We present this diffusion-approximation-based linear response

$$K_{x\lambda}^{\text{da}}(t, t') \equiv \frac{\delta}{\delta \lambda(t')} \left[\langle x[z; t] \rangle_{z \sim \mathcal{N}[\lambda(t), \lambda(t)]} \right] \quad (34)$$

alongside the true response to intensity modulations in Fig. 3. To this end, we simulate Eq. (32) but with the Gaussian process above replacing η and simultaneously modulate both the mean and the noise intensity (results shown in Fig. 3 as gray dashed lines). For the parameters that we have chosen, the diffusion approximation turns out to be a reasonable description of the susceptibility, although in the case of low input intensity and high amplitudes [panel (a)], somewhat stronger deviations become apparent.

The validity of Eq. (10) and thereby Eq. (12) relies on the Poissonianity of the input. To exemplify this, we generate non-Poissonian input processes with intensity $\lambda_0 + \varepsilon \nu(t)$, by first sampling a Poisson process with intensity $n [\lambda_0 + \varepsilon \nu(t)]$ and then keeping only every n 'th spike. As shown in Fig. 4(a), this procedure, in the absence of modulation $\varepsilon = 0$, decreases the coefficient of variation $C_v^2 = \langle \langle I^2 \rangle \rangle / \langle I \rangle^2 = 1/n$ (where $\langle \langle \cdot \rangle \rangle$ denotes a cumulant, i.e., here the variance) of the interspike interval I such that the so generated processes (for $n = 2, 3, \dots$) are more regular than a Poisson process ($C_v = 1$). For these processes, Eq. (12) is violated, as shown in Fig. 4(b). Moreover, no frequency-independent linear relation between $S_{x\eta}$ and χ can be found. The violation is most severe in a frequency band about the input intensity (black dotted line).

The deviation in Fig. 4(b) can be cured at low frequencies by using naively the color-correction Eq. (28), but remains at frequencies $\omega \gtrsim 2\pi\lambda_0$ [see Fig. 4(c)]. However, if the input process is truly a Cox process, as required in Sec. II B, the color-correction Eq. (28) seems to be a good approximation, see Fig. 5. Thus, the correlation-response

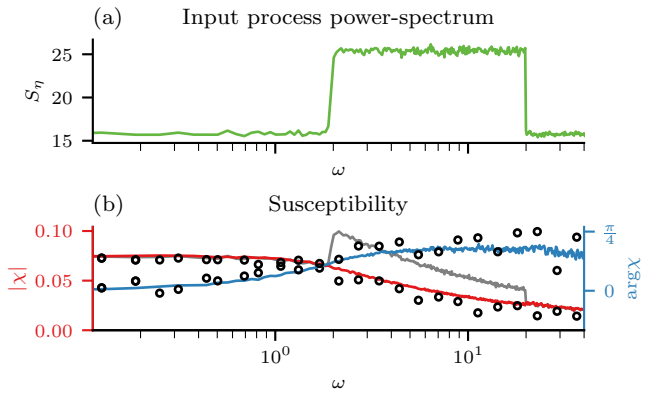


Figure 5. Test of the approximate CRR, Eq. (28), for a Cox-process-driven LIF neuron. (a) Power spectrum S_η of a Cox process, in which the intensity is band-pass Gaussian noise with mean $m(t) = 16$ and power spectrum $S_\lambda(\omega) = 10 \cdot \mathbf{1}_{2 < \omega < 20}$. (b) Absolute value (red) and argument (blue) of the right-hand side of Eq. (28), and respective susceptibility of the model Eq. (32) (black circles), obtained by stochastic simulations (App. A) using the stimulus $\varepsilon \cos(\omega_s t)$ with $\varepsilon = 0.2$. The gray line is the absolute value of the right-hand side of Eq. (12). Parameters: Time step $\Delta t = 10^{-3}$, integration time $T = 100$, $v_T = 1$, $v_R = 0.5$, $\mu = 0$, $\tau_s = 0$, $A = 0.05$.

K_C seems to be negligible for the model Eq. (32). In Sec. III C we find a situation in which Eq. (28) works for non-Cox noise, too.

2. Fluctuation-response relation

Next, we leverage Eq. (12) and follow the approach of [11], to derive a relation between the spontaneous output fluctuations of the model Eq. (32) and the output's response to modulations of the input intensity. To this end, we formally incorporate the reset mechanism into Eq. (32)

$$\dot{v} = -v + \mu + (\alpha * \eta) - (v_T - v_R)x(t). \quad (35)$$

Note that if the input would not be smoothed by α , the reset term would have to be $-[v(t) - v_R]x(t)$, as e.g. in Ref. [45], to account for overshooting. The product $v(t)x(t)$ would be inconvenient because it would lead to third-order statistics in the following expressions (a similar problem emerges when an absolute refractory period is taken into account [13]), which we avoid by using the synaptic filter, which is biophysically more plausible anyway. Following [11], we assume stationary statistics (i.e., $\lambda(t) = \lambda_0$), apply Rice's method to Eq. (35), and get for $\omega \neq 0$

$$S_{x\eta}(\omega) = \frac{(v_T - v_R)S_x(\omega) + (1 + i\omega)S_{xv}(\omega)}{\tilde{\alpha}^*(\omega)}, \quad (36)$$

where $\tilde{\alpha}(\omega) = A(1 - i\omega\tau_s)^{-2}$, the (cross-) power spectra $S_{FG}(\omega) = \langle \langle \tilde{F}(\omega) \tilde{G}^*(\omega) \rangle \rangle / T$ with the finite-time-

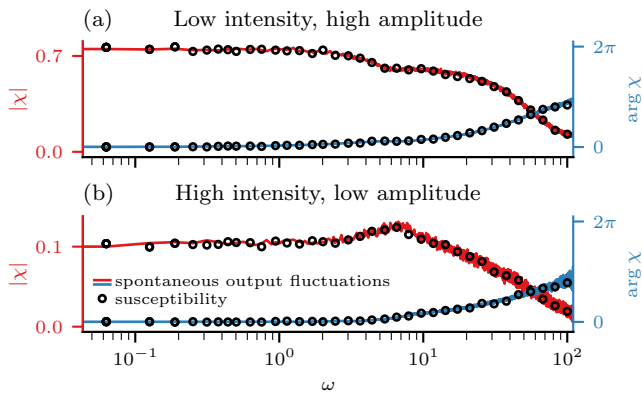


Figure 6. Test of the fluctuation-response relation, Eq. (37), for a constant baseline intensity λ_0 . (a) and (b) Susceptibility computed from spontaneous output fluctuations [right-hand side of Eq. (37)], absolute value (red) and argument (blue, right axis), and susceptibility computed by explicitly modulating the intensity (black circles, absolute value and argument respectively). The agreement of colored lines and black circles corroborates Eq. (37). The susceptibility computed by explicit modulations (black circles) is the same as in Fig. 3, but the colored lines here are exclusively *output* statistics. All statistics are measured in stochastic simulations, see App. A. Parameters as in Fig. 3, except for the spontaneous case in (b), here $\Delta t = 10^{-5}$ was necessary to achieve agreement.

window Fourier transform $\tilde{G}(\omega) = \int_0^T dt e^{i\omega t} G(t)$, and the asterisk denotes the complex conjugate.

Plugging Eq. (12) into Eq. (36) then yields a fluctuation-response relation (FRR)

$$\chi(\omega) = \frac{(v_T - v_R)S_x(\omega) + (1 + i\omega)S_{xv}(\omega)}{\lambda_0 \tilde{\alpha}^*(\omega)}. \quad (37)$$

Thus, the susceptibility can be computed using exclusively output fluctuations, quantified by S_x and S_{xv} , and without knowing the input spike times (although λ_0 and α must still be known). Eq. (37) is tested and confirmed in Fig. 6.

3. A non-stationary case

While many tools for stochastic systems are tailored to stationary situations, in a number of areas, such as climate research or biology, non-stationary behavior cannot be ignored without losing key features of the dynamics. For instance, the model Eq. (32) does not approach stationarity if the baseline rate $\lambda(t)$ is not constant. If $\lambda(t)$ varies sufficiently slowly, one would not expect strong differences from a stationary setting. Indeed, as we show in Fig. 7, when incorporating a slow Gaussian pulse $\lambda(t) = \lambda_{01} + \lambda_{02} \exp[-(t-t_m)^2/(2\sigma^2)]$ into the baseline intensity, the system's output rate adapts adiabatically to the changing input intensity. This is reflected by the scale invariance of the output rate with respect to the pulse width σ , see the overlapping gray lines in Fig. 7(a).

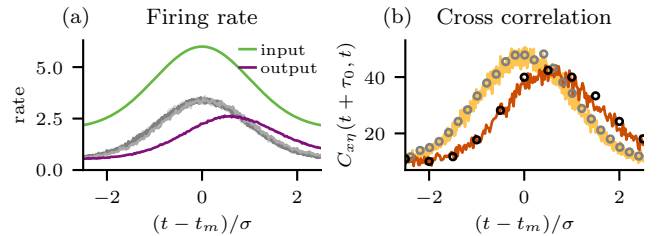


Figure 7. LIF neuron model: Test of the Eq. (10) for non-stationary dynamics. (a) Output firing rate (gray and purple) of Eq. (32) for a time-dependent input intensity $\lambda(t) = 2 + 4 \exp[-(t-t_m)^2/(2\sigma^2)]$ (green) for $\sigma = 10$, $\sigma = 5$, and $\sigma = 1$ (overlapping gray lines) and $\sigma = 0.1$ (purple line). (b) Cross-correlation $C_{x\eta}(t + \tau_0, t)$ with $\tau_0 = 0.05$ for $\sigma = 5$ (yellow line) and $\sigma = 0.1$ (orange line), and response function $\lambda(t)K(t + \tau_0, t)$ for $\sigma = 5$ (gray circles) and $\sigma = 0.1$ (black circles). Furthermore $v_T = 1$, $v_R = 0.5$, $\mu = 0$, and $\tau_s = 0.02$.

Thus, non-surprisingly, the non-stationary CRR Eq. (10) is fulfilled for the adiabatic case [yellow line and gray circles agree in Fig. 7(b)]. Truly interesting non-stationary behavior is achieved, when the pulse is too short to be responded to adiabatically, see the purple line in Fig. 7(a), which breaks the scale invariance (and also the symmetry w.r.t. the pulse center t_m). However, as we confirm for $\sigma = 0.1$, Eq. (10) is still valid in this non-adiabatic case [orange line and black circles agree in Fig. 7(b)].

C. Recurrent neural network

Here, we discuss the problem of stimulating a ‘control’ neuron in a network to achieve a desired time-dependent firing rate in a ‘target’ neuron. If the susceptibility of the control neuron χ_{cI} to a current injection $I(t)$ is known and spontaneous measurements of pair-wise cross-correlations have been conducted, one can apply the approximate CRR for colored shot noise Eq. (28) to estimate the remote susceptibility

$$\chi_{tI}(\omega) \approx S_c(\omega)^{-1} S_{tc}(\omega) \chi_{cI}(\omega), \quad (38)$$

where S_c is the power spectrum of the control neuron and S_{tc} is the cross-spectrum between the target- and the control neuron. Knowledge of χ_{tI} then allows one to make the target fire with a desired rate $r_t(t)$ by applying the current

$$I(t) = \mathcal{F}^{-1} [\mathcal{F}[r_t]/\chi_{tI}](t) \quad (39)$$

to the control neuron. Note that beside the assumptions for Eq. (28), one also needs to assume that the control and the target neuron receive independent noise from the rest of the network (see Sec. II A). This can be violated in dense networks, but, as we show next, for the biologically relevant case of sparse neural networks the assumption is justified.

For concreteness, we consider a sparsely connected random neural network [41]. This network model consists

of N_E excitatory and $N_I = N_E/4$ inhibitory LIF neurons. Each neuron has exactly C_E incoming excitatory synapses with efficacy J , and C_I incoming inhibitory synapses with efficacy $-gJ$. Thus the evolution of the network is given by

$$\begin{aligned} \dot{v}_i = & -v_i + J \sum_{j \in C_E(i)} x_j(t) - gJ \sum_{j \in C_I(i)} x_j(t) \\ & + J \sum_{j=1}^{C_E} x_{\text{ext},j}^i, \end{aligned} \quad (40)$$

with the additional fire-and-reset rule as in Eq. (32). Here, $x_{\text{ext},j}^i$ are independent external Poisson processes with intensity ν_{ext} and $C_E(i)$ [$C_I(i)$] is the set of excitatory [inhibitory] neurons that send spikes to neuron i .

In Fig. 8, we show simulation results for this network. We selected two neurons as control and target respectively, enforcing that the target is at one-synapse distance from the control [highlighted by the green arrow in Fig. 8(a)]. The susceptibilities χ_{cI} and χ_{tI} are obtained from simulations in which the control neuron was directly stimulated with a Gaussian white noise current. The cross-spectrum S_{tc} and the power spectrum S_c are obtained from spontaneous simulations. As shown in Fig. 8(b) and (c), the estimate Eq. (38) captures the susceptibility quite well. In Fig. 8(d), we then demonstrate how χ_{tI} can be exploited to control the target indirectly: Here, we generate a Gaussian broadband stimulus $r_t(t)$ (turquoise line) with cut-off frequency $\omega_c = 2$, feed the current Eq. (39) to the control neuron, and observe the firing rate (purple line) of the target neuron. Note that the parameters here are chosen such that for a reasonable membrane time constant $\tau_m = 10$ ms, the spontaneous rate in dimensional units is ≈ 7 Hz, which is biologically reasonable.

IV. FURTHER VARIANTS OF THE CRR

Here we discuss two further variants of the CRR: First we show how to include random amplitudes of the input spikes, then we show CRRs for higher-order input-output cross-correlation functions and nonlinear response functions. Given the characteristic functional $Z_{\mathbf{p}}[u]$ of the input process, where \mathbf{p} denotes the (time-dependent) parameters of the noise model, CRRs can be found systematically by recognizing that they correspond to relations between functional derivatives of $Z_{\mathbf{p}}[u]$ w.r.t. $u(t)$ and functional Taylor coefficients of $Z_{\mathbf{p}}[u]$ w.r.t. parameters p_i . This is analogous to the derivations of Eq. (10) and Eq. (22) and will be exemplified for the two further cases below.

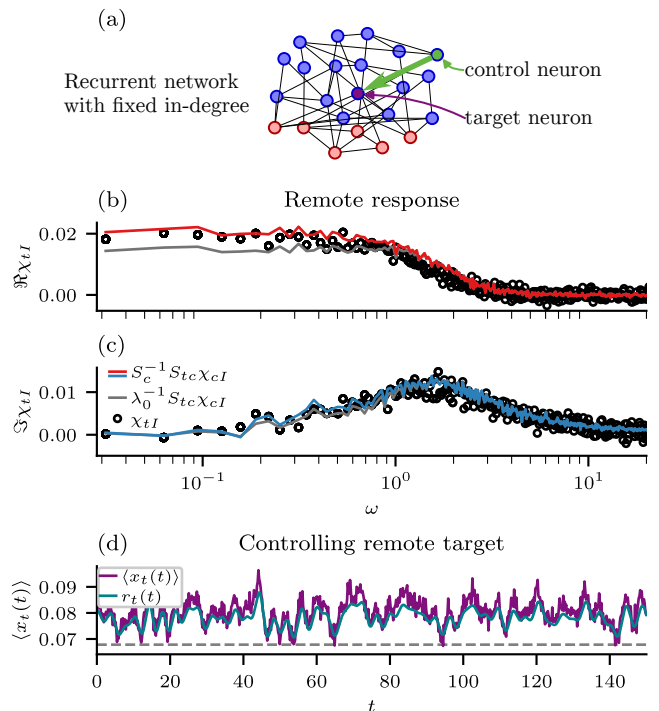


Figure 8. Remote control in recurrent neural networks. (a) Network model Eq. (40). One random neuron is selected as ‘control’ neuron, another random neuron is selected as ‘target’ neuron, constrained to be at one synapse distance from control (green arrow). The control neuron receives the current $I(t)$ in Eq. (39) to make the target fire with a desired rate $r_t(t)$. (b) and (c) Real- and imaginary part of the target’s response to control stimulation measured by stimulation (black circles) and estimated from Eq. (38) (red and blue lines). The gray line shows the estimate based on Eq. (12), i.e. without the color correction Eq. (28). (d) Desired rate $r_t(t)$ (turquoise line) and achieved rate (purple line) of the target neuron after application of the current Eq. (39) to the control neuron. The spontaneous rate of the target neuron is $r_0 \approx 0.68$ (gray dashed line). Parameters: $N_E = 10^5$, $N_I = 2.5 \cdot 10^4$, $C_E = 200$, $C_I = 50$, $g = 4.2$, $J = 0.01$, $\nu_{\text{ext}} = 0.83/(JC_E)$. The spectral measures in (b) and (c) are averaged over 10^4 noise realizations and the rate in (d) is averaged over 10^3 noise realizations. In both cases, the network realization is fixed. For a membrane time-constant of $\tau_m = 10$ ms, the y-ticks in (d) are 7 Hz, 8 Hz, and 9 Hz respectively.

A. Random amplitudes of input spikes

As a first variant, we consider an input process with random amplitudes $\eta(t) = \sum_i a_i \delta(t - t_i)$ where t_i are Poisson events with intensity λ_0 and a_i are independently sampled from an exponential distribution $p(a) = \Theta(a)b^{-1} \exp(-a/b)$. Thus, we replace the Poissonian input with a *marked* Poisson process. In the example of the shot-noise-driven LIF neuron, random amplitudes are a more faithful description of synaptic inputs that display considerable variability [26, 49–51]. Note that while one could ascribe the random amplitudes to an additional

random process as described in Sec. II A, specifically $\eta(t) = \xi(t)\eta_0(t)$, where η_0 is the unmarked Poisson process and $\xi(t) \stackrel{\text{i.i.d.}}{\sim} \Theta[\xi(t)]b^{-1} \exp[-\xi(t)/b]$, where independence refers to the time argument, the CRR Eq. (10) only applies to relations between the output and η_0 , whereas here we study the relation between the output and the full marked input $\eta(t)$.

The mean of the input process is $\langle \eta(t) \rangle = b\lambda_0$, thus modulating λ_0 and b has a similar effect on the mean input. In [26], the susceptibility $\chi(\omega)$ of a LIF neuron to an intensity modulation of such an input process has been derived. To fully explain the input-output cross-spectrum $S_{x\eta}(\omega)$ it turns out that $\chi(\omega)$ is not sufficient. Specifically, we show that one also needs the susceptibility $\chi_b(\omega)$ to time-dependent modulations of b .

Our starting point is the characteristic functional of an independently and identically marked Poisson process [52]

$$Z_{\lambda,b}[u] = e^{\int \lambda(t')[\phi_b(u(t'))-1]dt'}, \quad (41)$$

where $\phi_b(u) = \langle e^{iau} \rangle$ is the characteristic function of the marks (here amplitudes). For exponentially distributed amplitudes, $\phi_b(u) = 1/(1-iub)$. Similarly to Eq. (9), $C_{x\eta}$ can be expressed by a functional derivative $D(t) \equiv \frac{\delta}{\delta iu(t)} Z_{\lambda,b}[u]$, and similarly to Eq. (7), the two linear-response functions can be expressed by functional Taylor coefficients $T(t) \equiv \frac{\delta}{\delta \Lambda(t)} Z_{\Lambda,b}[u] \Big|_{\Lambda=\lambda}$ and $T_b(t) \equiv \frac{\delta}{\delta B(t)} Z_{\lambda,B}[u] \Big|_{B=b}$. Due to the identity (easily checked by insertion)

$$\frac{\partial}{\partial iu} \phi_b(u) = b\phi_b(u) + b^2 \frac{\partial}{\partial b} \phi_b(u), \quad (42)$$

the three functions D , T , and T_b are directly related

$$D(t') = \lambda b T(t') + b^2 T_b(t'), \quad (43)$$

as follows by straight forward differentiation. If we integrate Eq. (43) with $\int \mathcal{D}u y[u, t] \times$ and assume stationarity, we find for $\omega \neq 0$ the CRR

$$S_{x\eta}(\omega) = \lambda_0 b \chi(\omega) + b^2 \chi_b(\omega). \quad (44)$$

Thus, in the case of random amplitudes, the spontaneous input-output cross-spectrum is connected to *two* mechanistic properties of the system, the linear responses to intensity- and amplitude modulations, respectively.

The CRR, Eq. (44), is verified and illustrated in Fig. 9 for two opposite cases of the input process. The cross-spectrum decreases monotonically with frequency and saturates at a non-vanishing level, corresponding to the event that an input spike triggers immediately an output spike; this is more likely for larger amplitudes [saturation is larger in (a) than in (c)] and relies on our choice of a vanishing filter time $\tau_s = 0$. We also illustrate in Fig. 9 the relevance of the two contributions in Eq. (44), which agree for small frequencies but deviate otherwise, especially pronounced in the phase for large amplitudes and intermediate frequencies (b).

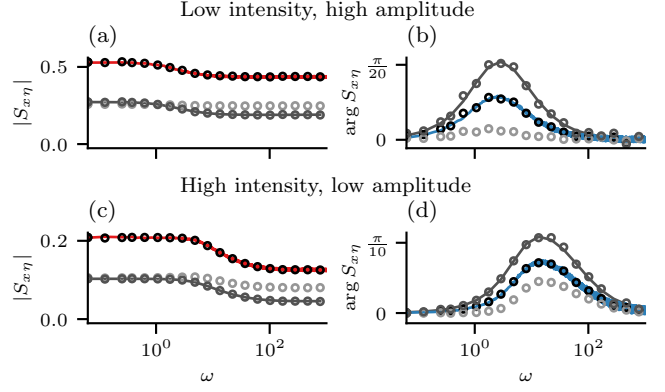


Figure 9. LIF neuron model: Test of the CRR for a LIF neuron driven by a Poisson process input with random amplitudes Eq. (44). Absolute value [(a) and (c), red lines] and argument [(b) and (d), blue lines] of the cross-spectrum $S_{x\eta}(\omega)$. Right-hand side of Eq. (44) (black circles) and single contributions $b^2\chi_b(\omega)$ (light gray circles) and $\lambda_0 b\chi(\omega)$ (dark gray circles); for the latter, the exact result [26] is shown (dark gray line), for all other lines and symbols, the statistics are measured in stochastic simulations, see App. A. Parameters: $v_T = 1$, $v_R = 0.5$, $\mu = 0$, and $\tau_s = 0$. For (a) and (b) $\lambda_0 = 2$, $b = 0.4$; and for (c) $\lambda_0 = 24$, $b = 1/20$.

B. Higher-order statistics and nonlinear response

Lastly, we demonstrate a higher-order CRR involving nonlinear response functions and higher-order cross-correlations. It has been recently suggested [53] that the nonlinear response of sensory cells may be important in certain detection problems [54]. Furthermore, taking into account nonlinear response overcomes the limitations of linear response theory of neural activity [55] and may exhibit surprising features already for simple neuron models [56].

Considering again a fixed-amplitude inhomogeneous Poisson process, the third input-output cumulant $C_{x\eta\eta}(t, t', t'') = \langle \langle x(t)\eta(t')\eta(t'') \rangle \rangle$ can be attributed to a linear combination of the linear-response function $K(t, t')$ and the second order response function $K_2(t, t', t'') = \frac{\delta^2}{\delta \varepsilon_s(t') \delta \varepsilon_s(t'')} \langle x[\eta; t] \rangle \Big|_{\varepsilon=0}$. Analogously to the above derivation, expressing $C_{x\eta\eta}$, K_2 , and K as path integrals including the second functional derivative of the characteristic functional of η and its second- and first functional Taylor coefficients w.r.t. the intensity, respectively, we find by comparing the integrands

$$C_{x\eta\eta}(t, t', t'') = \delta(t' - t'') \lambda(t') K(t, t') + \lambda(t') \lambda(t'') K_2(t, t', t''). \quad (45)$$

This strikingly simple relation reveals that the third-order cross-correlations are entirely determined by first- and second-order response functions. Similarly, cross-correlations of order n are given in terms of response functions up to order $n - 1$. Likewise, cross-correlations including orders $m \geq 2$ of x are related to response func-

tions of $\prod_{i=1}^m x(t_i)$.

V. SUMMARY AND OUTLOOK

In this paper, we derived a number of exact relations between the input-output cross-correlations of a shot-noise-driven system and its response functions. These CRRs can be regarded as analogues of the famous Furutsu-Novikov theorem for systems driven by Gaussian noise but are, as we demonstrated, not the same. Our theorem, holding true for the case of Poissonian shot noise (and in an extension for Cox noise), applies to simple functionals such as a linear filter but also to a more complicated system such as an excitable neuron that itself generates spikes (i.e. another shot noise process). We tested the basic relation for a particle detector and for a shot-noise-driven integrate-and-fire neuron and demonstrated that it is nontrivial, as it is not obeyed if the input shot noise deviates from Poisson statistics. We used the CRR for this model class to derive a novel FRR in the presence of shot noise. In a recurrent network we used the CRR to extract remote-response functions from spontaneous cross-correlations. Finally, we generalized the relation in two further respects: i) we replaced the common Poissonian input noise by a marked Poisson process, for which amplitudes are drawn from an exponential distribution; and ii) we exemplified how higher-order cross-correlation functions of shot-noise-driven systems can be related to higher-order response functions.

The approaches developed here enable the derivation of families of non-trivial input-output relations of systems driven by random series of events. It is conceivable, for instance, that the generalizations outlined above may be combined, i.e. we could consider a marked *and* doubly stochastic process as an input and also derive higher-order relations in this setting. Another extension is the common situation that a system is subject to several independent shot-noise processes or to both shot noise and Gaussian noise. In neurons, for instance, there are excitatory and inhibitory synaptic inputs and, moreover, several competing types of noise, some of which can be approximated by Gaussian noise, e.g. the channel noise from a large population of independent ionic channels [57]. We expect that in such cases, families of relations between various input-output cross-correlations and response functions to various modulations (e.g. intensities of excitatory and inhibitory input spike trains; mean and variance of Gaussian input noise) can be found and may serve to derive, for instance, corresponding families of FRRs. Another interesting model class for neural activity is the Hawkes process [55, 58, 59], which our study does not cover due to its deviation from Poissonian input statistics. It is thus an open problem to derive CRRs for this situation.

Regarding the specific application of the CRR to the integrate-and-fire model, several remarks are in order. First of all, analytical results for this model class are

scarce, and the CRRs may allow us to derive new exact results. For the case of random amplitudes, the intensity response is known, see [26], and the response to modulations of the amplitude might be obtained by the methods therein; knowing both of these functions would provide us with an explicit expression for the input-output cross-correlation function of this model. Secondly, the CRR can also be applied to more involved nonlinear models, such as integrate-and-fire models with adaptation [60–63], with synaptic short-term plasticity (see e.g. [64–68]), or with conductance-based input shot noise [69–73]. Beyond the integrate-and-fire framework, CRRs may be exploited in detailed biophysical models such as Hodgkin-Huxley-type neuron models with a true spike-generating mechanism, and spatially extended neuron models based on cable theory with stochastic inputs distributed over the neuron’s dendrite [74, 75]. Thirdly, at the network level, input-output cross-correlations are particularly relevant, because the input spikes for one neuron are another neuron’s output spikes, and modern multi-electrode arrays allow for parallel recording of hundreds to thousands of spike trains. Expanding on the approach worked out in Sec. III C, we may use the CRR to determine an entire matrix of pair-wise response functions in heterogeneous networks of spiking neurons. Furthermore, from a more theoretical point of view, CRRs can be helpful by constraining the constituents in the theory of neural networks. For example, in a recent cavity-method approach to rate-based neural networks [12] with Gaussian statistics, the Gaussian FNT was used to connect neural cross-correlations and response functions. With the results presented here, such approaches can likely be extended to recurrent networks of spiking neurons. Last but not least, in the theory of neural learning, the important paradigm of spike-timing dependent plasticity involves the cross-correlation of pre- and post-synaptic spike trains. Relations such as the CRR constrain the possible dynamics of the synaptic weights during learning and may thus be instrumental to understand this type of self-organization in the brain.

ACKNOWLEDGMENTS

We are grateful to Igor Sokolov for helpful discussions. This work has been funded by the Deutsche Forschungsgemeinschaft (DFG, German Research Foundation), SFB1315, project-ID 327654276 to BL.

Appendix A: Numerical methods

The main results of this manuscript are links between correlation functions and response functions, both of which are in general hard to obtain analytically. Therefore, in Figs. 2–9, we compute these statistics from stochastic simulations. This involves sampling a large number of realizations of the input processes, comput-

ing the respective output processes, and assuming that averages over the ensemble of input processes may be approximated by averages over the finite number of input realizations. In this appendix, we lay out technical details.

1. Generation of Poisson processes

To sample Poisson processes with intensity $\Lambda(t)$ we discretize time into timesteps Δt and perform a Bernoulli trial in each time bin k with $t_k = k\Delta t$ [52]. Specifically, we draw uniform random numbers $q_k \sim \mathcal{U}(0, 1)$ between 0 and 1. If $q_k \leq \Lambda(t_k)\Delta t$, we note an event at time t_k , thus the so-sampled Poisson process may be represented by the discrete-time spike-train

$$\eta_k = \sum_{k' \text{ s.t. } q_{k'} \leq \Lambda(t_{k'})\Delta t} \frac{\delta_{kk'}}{\Delta t}. \quad (\text{A1})$$

Here, the ratio of the Kronecker delta and the time step is the discrete-time approximation of the Dirac delta function in the continuous-time spike-train, $\eta(t) = \sum \delta(t - t_{k'})$.

2. Integration of Langevin equations

To sample the Ornstein-Uhlenbeck process Eq. (31), we integrate the Langevin equation using the Euler-Maruyama method. Specifically, we initialize the value of the process at time t_0 as $\zeta_0 = 0$ and then iteratively compute the subsequent values of the process

$$\zeta_{k+1} = \left(1 - \frac{\Delta t}{\tau_\zeta}\right) \zeta_k + \sqrt{2\sigma_\zeta^2 \frac{\Delta t}{\tau_\zeta}} z_k, \quad (\text{A2})$$

where $z_k \stackrel{\text{i.i.d.}}{\sim} \mathcal{N}(0, 1)$. To get rid of transient behavior due to the choice of ζ_0 , we cut off a transient time $T_{\text{warm}} = 50 \gg \tau_\zeta = 1$.

The same type of integration is applied to simulate the LIF dynamics Eq. (32) driven by white Gaussian noise $z(t)$ Eq. (33) in order to determine the diffusion approximation of the response function Eq. (34). Here, we apply a Markovian embedding to implement the filter $\alpha(t)$ by means of two additional auxiliary variables m_1 and m_2

$$\begin{aligned} (\alpha * \eta)(t) &\approx (\alpha * z)(t) = Am_1(t)/\tau_s^2 \\ \dot{m}_1(t) &= -\tau_s^{-1}m_1(t) + m_2(t) \\ \dot{m}_2(t) &= -\tau_s^{-1}m_2(t) + z(t). \end{aligned} \quad (\text{A3})$$

The last line describes again an Ornstein-Uhlenbeck process that can in discrete time be simulated as in Eq. (A2).

3. Sampling colored Gaussian noise

For the production of Fig. 5, we use a different method [76, and references therein] to sample the Gaussian input

process. Namely, we generate the Gaussian noise $\lambda(t)$ with given mean m and power spectrum $S_\lambda(\omega)$ by sampling the Fourier transform $\tilde{\lambda}(\omega)$. Since we here consider a stationary random process, that is $\langle\langle \lambda(t + \tau)\lambda(t) \rangle\rangle$ is invariant to translations in time t , the correlations in frequency space are diagonal $\langle\langle \tilde{\lambda}(\omega)\tilde{\lambda}^*(\omega') \rangle\rangle \propto \delta(\omega - \omega')$. Thus, for a finite time window T and discrete frequency bins $\omega_k = 2\pi k/T$, we may conveniently sample $|\tilde{\lambda}(\omega_k)| \sim \mathcal{N}[\tilde{m}(\omega_k), S_\lambda(\omega_k)]$ and $\arg[\tilde{\lambda}(\omega_k)] \sim \mathcal{U}(0, 2\pi)$ independently for each frequency bin. Lastly we apply the inverse Fourier transform to obtain $\lambda(t)$.

4. Integrating LIF neurons

To integrate the LIF neuron Eq. (32), we first sample the input as detailed above, and then integrate Eq. (32) with a simple forward scheme. Specifically, at each step k , the membrane voltage is updated as

$$v_{k+1} = v_k + \Delta t [-v_k + \mu + (\alpha * \eta)(t_k)] \quad (\text{A4})$$

and the convolution $\alpha * \eta$ is computed in advance. Alternatively, the Markovian embedding Eq. (A3) could be used for shot noise $\eta(t)$ instead of $z(t)$, too.

5. Spontaneous statistics

For spontaneous statistics, e.g. the left-hand sides in Eqs. (10), (22), (37), and (44), the simulations are computed as outlined above for large numbers of input realizations. Per realization, the correlation functions and spectra correspond to simple products (of Fourier transforms) of variables. The presented statistics are averages of these per-realization products over all realizations.

6. Response functions

The susceptibility χ of a variable $\langle x \rangle$ to modulations of a parameter λ_0 is computed as follows. For each frequency ω_s at which the susceptibility is sought, we simulate the dynamics of x for many realizations of the input with parameter $\lambda_0 + \varepsilon \cos(\omega_s t)$. Assuming stationary dynamics for $\varepsilon = 0$, linear response theory states that for $\omega_s > 0$

$$\langle \tilde{x}(\omega) \rangle = \varepsilon \pi \chi(\omega) \delta(\omega - \omega_s) + \mathcal{O}(\varepsilon^2). \quad (\text{A5})$$

Thus, for each ω_s we may extract the susceptibility $\chi(\omega_s) = [\Delta\omega/(\varepsilon\pi)] \langle \tilde{x}(\omega_s) \rangle$, where the average is taken over the realizations and the frequency step is given in terms of the simulation window T as $\Delta\omega = 2\pi/T$.

Appendix B: CRR implies white-noise FNT in the diffusion limit

Here, we show that the CRR Eq. (10) implies the FNT for white Gaussian noise. To this end, we follow an approach put forward by [77, 78] to recall that every white Gaussian noise process can be regarded as the diffusion limit of a scaled Poisson process with offset. Thus, the CRR which applies to Poisson processes has a corresponding property which applies to white Gaussian noise; this property turns out to be the FNT.

The diffusion approximation in its common use refers to replacing an inhomogeneous Poisson process by white Gaussian noise with matched time-dependent mean and noise intensity. This replacement neglects all cumulants of order $k \geq 3$ of the Poisson process. However, the scaled Poisson process with offset

$$z_n(t) = a_n \eta_n(t) + \psi_n(t), \quad (\text{B1})$$

where $\eta_n(t)$ is a Poisson process with intensity $\lambda_n(t)$, becomes equivalent to white Gaussian noise

$$x[z_n; t] \xrightarrow{n \rightarrow \infty} x[\xi; t], \quad (\text{B2})$$

in the sense specified in [77, 78], in a specific limit. If

$$\begin{aligned} \lambda_n(t) &= A(t)n + B(t)n^2, \\ a_n &= a_{\dagger}/n, \\ \psi_n(t) &= -a_{\dagger}B(t)n, \end{aligned} \quad (\text{B3})$$

with A , B , and a_0 independent of n , then in the limit $n \rightarrow \infty$ the mean and autocorrelation of z are finite, namely $\langle z(t) \rangle = a_{\dagger}A(t)$ and $\langle \langle z(t)z(t') \rangle \rangle = a_{\dagger}^2 B(t)\delta(t-t')$, yet all cumulant functions of order $k \geq 3$ vanish $\propto 1/\mathcal{O}(n^{k-2})$. Thus, in this limit, Eq. (B1) is statistically identical to a white Gaussian process ξ with mean $m(t) = a_{\dagger}A(t)$ and noise intensity $D(t) = a_{\dagger}^2 B(t)$. Conversely, every white Gaussian noise process can be represented as the diffusion limit of a scaled Poisson process with offset.

Modulating the intensity of the Poisson process, specifically replacing $\lambda_n(t)$ by $\lambda_n(t) + \varepsilon s_n(t)$ with $s_n(t) = s_{\dagger}(t)n$, corresponds in the limit $n \rightarrow \infty$ to modulating the mean of the Gaussian process, i.e. replacing $m(t)$ by $m(t) + \varepsilon \hat{s}(t)$ with $\hat{s}(t) = a_{\dagger} s_{\dagger}(t)$, whereas the noise intensity is not affected. Thus, the linear response K_n of a functional $x[\eta_n; t] \equiv \hat{x}[z_n = a_n \eta_n + \psi_n; t]$ to modulation of $\lambda_n(t)$,

$$\begin{aligned} \langle x[\eta_n; t] \rangle_{\varepsilon} &= \langle x[\eta_n; t] \rangle_0 \\ &+ \varepsilon \int dt' K_n(t, t') s_n(t') + \mathcal{O}(\varepsilon^2), \end{aligned} \quad (\text{B4})$$

corresponds in the diffusion limit to the response of \hat{x} to modulating $m(t)$

$$\begin{aligned} \langle \hat{x}[\xi; t] \rangle_{\varepsilon} &= \lim_{n \rightarrow \infty} \langle \hat{x}[z_n; t] \rangle_{\varepsilon} \\ &= \langle \hat{x}[\xi; t] \rangle_0 + \lim_{n \rightarrow \infty} \frac{\varepsilon}{a_n} \int dt' K_n(t, t') \hat{s}(t') + \mathcal{O}(\varepsilon^2), \end{aligned} \quad (\text{B5})$$

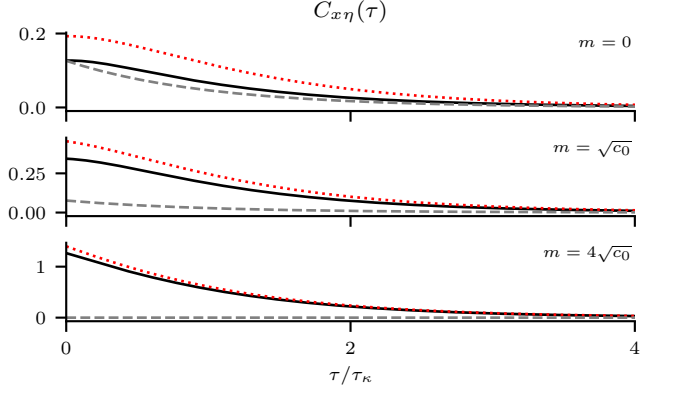


Figure 10. Violation of the CRR for Cox processes with non-Gaussian intensity due to the non-negativity constraint. Input-output cross-correlation Eq. (C10) of a linear filter driven by Cox noise with Gaussian intensity that is clipped at zero (black line). Right-hand side of Eq. (22) with the response functions Eqs. (C7) and (C9) (red dotted line). The disagreement between red and black lines displays a violation of the CRR Eq. (22). Contribution of the variance-response to the right-hand side of Eq. (22), $2c_0 K_{xC_\phi}(\tau)$ (gray dashed line). Parameters: $\tau_\kappa = 4$, $\tau_\phi = 2$, $c_0 = 0.1$, and m is varied as indicated in the legend.

where ξ is the Gaussian noise introduced above. Thus the linear response function to mean modulations of the Gaussian process is $K_{x\xi} = \lim_{n \rightarrow \infty} K_n/a_n$ in the diffusion limit. Additionally, the cross-correlations $C_{x\eta}(t, t') = \langle \langle x(t)\eta_n(t') \rangle \rangle$ and $C_{\hat{x}\xi}(t, t') = \langle \langle \hat{x}(t)\xi(t') \rangle \rangle$ are related by $C_{\hat{x}\xi} = a_n C_{x\eta}$ in the diffusion limit. Thus, Eq. (10) implies the white-noise case of the Gaussian FNT Eq. (11)

$$\begin{aligned} C_{\hat{x}\xi}(t, t') &= a_n^2 \lambda_n(t') K_{x\xi}(t, t') \\ &= D(t') K_{x\xi}(t, t'), \end{aligned} \quad (\text{B6})$$

since $a_n^2 \lambda_n(t) = \frac{a_{\dagger}^2}{n^2} (A(t)n + B(t)n^2) \xrightarrow{n \rightarrow \infty} a_{\dagger}^2 B(t) \equiv D(t)$.

Appendix C: Impact of non-negativity

In Sec. II B we discuss the Cox process, i.e. a conditionally Poissonian point process $\eta(t)$ with intensity $\lambda(t)$, and $\lambda(t)$ is itself a random process. Specifically, we choose $\lambda(t) \equiv \Theta[\phi(t)]\phi(t)$ where $\phi(t)$ is a Gaussian process with mean $m(t)$ and autocorrelation function $C_\phi(t, t')$. In the derivation of the extended form of the CRR for this Cox process, Eq. (22), we assume that $\phi(t)$ is almost always non-negative, i.e. that the positive mean value is much larger than the standard deviation. We may thus set $\lambda(t) = \phi(t)$. This allows us to achieve the closed-form expression of the characteristic functional $\langle \exp[\int \lambda[\phi(t)] (e^{iu(t)} - 1) dt] \rangle_\phi$, see Eq. (16). Nonlinearities of $\lambda(\phi)$ could be captured systematically by expressing λ as a polynomial around m , taking the contributions up to and including $\mathcal{O}[(\phi - m)^2]$ into account by absorbing it into the Gaussian problem, and

treating higher order non-linearities of λ using Feynman diagrams. However, such a procedure is likely to become cumbersome.

Setting $\lambda = \phi$ is legitimate if the probability of negative ϕ ,

$$\mathbb{P}(\phi < 0) = \frac{1}{2} \operatorname{erfc}[m(t)/\sqrt{2C_\phi(t,t)}], \quad (\text{C1})$$

can be neglected (here erfc is the complementary error function). To estimate the impact of the non-negativity constraint on the validity of the CRR Eq. (22), we first show that Eq. (22) is fulfilled for a linear system if indeed $\lambda = \phi$. Second, we show how Eq. (22) is violated for a linear system if $\mathbb{P}(\phi < 0) \ll 1$ is violated.

Assuming $\phi = \lambda$, the response functions of a linear filter $x[\eta; t] = \int_0^\infty d\tau \kappa(\tau) \eta(t - \tau)$ can be computed explicitly. Since here, $\langle \eta(t) \rangle = \langle \lambda(t) \rangle = m(t)$, and thus $\langle x(t) \rangle = \int_0^\infty d\tau \kappa(\tau) m(t - \tau)$, the linear response functions to mean- and autocorrelation modulations are

$$K_{xm}(t, t') = \frac{\delta}{\delta m(t')} \langle x(t) \rangle = \Theta(t - t') \kappa(t - t') \quad (\text{C2})$$

and

$$K_{xC_\phi}(t, t', t'') = \frac{\delta}{\delta C_\phi(t', t'')} \langle x(t) \rangle = 0. \quad (\text{C3})$$

The fact that $K_{xC_\phi} \equiv 0$ shows that for $\mathbb{P}(\phi < 0) \ll 1$, a linear system does not respond to modulations of C_ϕ .

The input-output cross-correlation can also be computed explicitly

$$\begin{aligned} C_{x\eta}(t, t') &= \int_0^\infty d\tau \kappa(\tau) \langle \eta(t - \tau) [\eta(t') - m(t')] \rangle \\ &= m(t') \Theta(t - t') \kappa(t - t') \\ &\quad + \int dt'' \Theta(t - t'') \kappa(t - t'') C_\phi(t', t'') \\ &= m(t') K_{xm}(t, t') \\ &\quad + \int dt'' C_\phi(t', t'') [2K_{xC_\phi}(t, t', t'') + K_{xm}(t, t'')], \end{aligned} \quad (\text{C4})$$

where in the last step we have recast $C_{x\eta}$ into the form of the right-hand side of Eq. (22), using the above expressions for the response functions; Eq. (22) is thus explicitly confirmed for the linear system.

If $\mathbb{P}(\phi(t) < 0) \ll 1$ is violated, the above calculations do not provide a valid approximation anymore. The double-average $\langle f[\eta] \rangle$, where first the conditional average over Poisson processes η with intensity $\Theta(\phi)\phi$, and then the average over Gaussian processes ϕ have to be carried out, produces expectation values of a nonlinear function of Gaussian random variables. Yet, the two response functions can be computed explicitly from the mean output

$$\begin{aligned} \langle x(t) \rangle &= \int^t dt' \kappa(t - t') \langle \eta(t') \rangle \\ &= \int^t dt' \kappa(t - t') \bar{\eta}[m(t'), C_\phi(t', t')] \end{aligned} \quad (\text{C5})$$

where

$$\begin{aligned} \bar{\eta}(m, c) &= \langle \Theta(\phi)\phi \rangle_{\phi \sim \mathcal{N}(m, c)} \\ &= c \frac{1}{\sqrt{2\pi c}} e^{-m^2/(2c)} + \frac{m}{2} \operatorname{erfc}(-m/\sqrt{2c}) \end{aligned} \quad (\text{C6})$$

is the ensemble average of the input process. The linear response to mean modulations follows from differentiating Eq. (C5)

$$\begin{aligned} K_{xm}(t, t') &= \frac{\delta}{\delta m(t')} \int^t ds \kappa(t - s) \bar{\eta}[m(s), C_\phi(s, s)] \\ &= \frac{d}{dh} \int^t ds \kappa(t - s) \times \\ &\quad \times \bar{\eta}[m(s) + h\delta(s - t'), C_\phi(s, s)] \Big|_{h=0} \\ &= \Theta(t - t') \kappa(t - t') \frac{1}{2} \operatorname{erfc}[-m(t')/\sqrt{2C_\phi(t', t')}] \end{aligned} \quad (\text{C7})$$

For $C_\phi \rightarrow 0$ this reproduces Eq. (C2), since $\lim_{x \rightarrow -\infty} \operatorname{erfc}(x) = 2$.

Concerning modulations of $C_\phi(t, t')$, we first observe that the mean output Eq. (C5) only depends on the variance $V_\phi(t) \equiv C_\phi(t, t)$. Thus, the linear response to modulations of C_ϕ is given by the linear response to variance-modulations $K_{xC_\phi}(t, t', t'') = \delta(t' - t'') K_{xV_\phi}(t, t')$, as one can see by Taylor expanding Eq. (C5) and identifying the correlation response

$$\begin{aligned} \langle x(t) \rangle_\varepsilon &= \int^t dt' \kappa(t - t') \bar{\eta}[m(t'), V_\phi(t') + \varepsilon D(t', t')] \\ &= \langle x(t) \rangle_0 + \varepsilon \int^t dt' \kappa(t - t') \times \\ &\quad \times \frac{\partial}{\partial V_\phi(t')} \bar{\eta}[m(t'), V_\phi(t')] D(t', t') \\ &= \langle x(t) \rangle_0 + \varepsilon \int^t dt' \int^t dt'' \kappa(t - t') \times \\ &\quad \times \delta(t' - t'') \frac{\partial}{\partial V_\phi(t')} \bar{\eta}[m(t'), V_\phi(t')] D(t', t''). \end{aligned} \quad (\text{C8})$$

As one may read off from this, the variance-response follows again by differentiating Eq. (C5)

$$\begin{aligned} K_{xV_\phi}(t, t') &= \frac{\delta}{\delta V_\phi(t')} \int^t ds \kappa(t - s) \bar{\eta}[m(s), V_\phi(s)] \\ &= \Theta(t - t') \kappa(t - t') \frac{1}{2} \frac{1}{\sqrt{2\pi V_\phi}} e^{-m^2/(2V_\phi)}. \end{aligned} \quad (\text{C9})$$

Thus, as opposed to the case where $\mathbb{P}(\phi < 0) \ll 1$, the nonlinearity induces a non-vanishing response to variance modulations. This response function vanishes for $V_\phi \rightarrow 0$, the limit in which $\mathbb{P}(\phi < 0) \rightarrow 0$, provided that $m > 0$.

To test the violation of Eq. (22), we additionally need

to compute the input-output cross-correlation

$$\begin{aligned}
C_{x\eta}(t, t') &= \int^t ds \kappa(t-s) \langle \eta(s) \eta(t') \rangle \\
&\quad - \int^t ds \kappa(t-s) \langle \eta(s) \rangle \langle \eta(t') \rangle \\
&= \int^t ds \kappa(t-s) \times \\
&\quad \times [\langle \lambda[\phi(s)] \delta(s-t') \rangle + C_\lambda(s, t')] \\
&= \Theta(t-t') \kappa(t-t') \bar{\eta}[m(t'), V_\phi(t')] \\
&\quad + \int^t ds \kappa(t-s) C_\lambda(s, t').
\end{aligned} \tag{C10}$$

We are not aware of a closed form expression for C_λ in terms of C_ϕ , although a possible method is applied in

[79]. Here, we content ourselves with computing C_λ numerically for the special case $C_\phi(t, t') = c_0 e^{-|t-t'|/\tau_\phi}$ by evaluating the double integral

$$\begin{aligned}
C_\lambda(\tau) &= \int d\phi_1 d\phi_2 \mathcal{N} \left[\begin{pmatrix} \phi_1 \\ \phi_2 \end{pmatrix} \middle| \begin{pmatrix} m \\ m \end{pmatrix}, \begin{pmatrix} c_0 & c_\tau \\ c_\tau & c_0 \end{pmatrix} \right] \times \\
&\quad \times [\lambda(\phi_1) - \bar{\eta}(m, c_0)] [\lambda(\phi_2) - \bar{\eta}(m, c_0)],
\end{aligned} \tag{C11}$$

where $c_\tau = C_\phi(\tau)$, using Gauss-Hermite quadrature.

In Fig. 10 we show the input-output cross-correlation Eq. (C10) as well as the right-hand side of Eq. (22) using the response functions Eqs. (C7) and (C9) for $\kappa(\tau) = e^{-\tau/\tau_\kappa}$ and different values of the coefficient of variation $\sqrt{c_0}/m$. As expected, the CRR Eq. (22) is violated if $\sqrt{c_0}/m$ is not small enough, corresponding to $\mathbb{P}(\phi < 0) \ll 1$ being violated.

-
- [1] C. Gardiner, *Handbook of Stochastic Methods for Physics, Chemistry, and the Natural Sciences*, Proceedings in Life Sciences (Springer, 1985).
- [2] W. Schottky, Über spontane Stromschwankungen in verschiedenen Elektrizitätsleitern, *Ann. Phys.* **362**, 541 (1918), translated in [80].
- [3] W. Gerstner, W. Kistler, R. Naud, and L. Paninski, *Neuronal Dynamics: From Single Neurons to Networks and Models of Cognition* (Cambridge University Press, 2014).
- [4] S. Tesfamariam and K. Goda, *Handbook of Seismic Risk Analysis and Management of Civil Infrastructure Systems*, Woodhead Publishing Series in Civil and Structural Engineering (Elsevier Science, 2013).
- [5] K. Furutsu, On the statistical theory of electromagnetic waves in a fluctuating medium (1), *Res. Natl. Bur. Stand. D* **67D**, 303 (1963).
- [6] E. A. Novikov, Functionals and the random-force method in turbulence theory, *J. Exp. Theor. Phys.* **20**, 1290 (1965).
- [7] U. Frisch, *Turbulence: The Legacy of A. N. Kolmogorov* (Cambridge University Press, 1995).
- [8] Y. V. Tarasov and O. M. Stadnyk, Effect of anderson localization on surface plasmon polariton propagation and outward leakage when scattered by a randomly corrugated section of the interface, *Phys. Rev. B* **108**, 214202 (2023).
- [9] J. A. Krommes, Fundamental statistical descriptions of plasma turbulence in magnetic fields, *Phys. Rep.* **360**, 1 (2002).
- [10] L. Bentkamp, T. D. Drivas, C. C. Laescu, and M. Wilczek, The statistical geometry of material loops in turbulence, *Nat. Commun.* **13**, 2088 (2022).
- [11] B. Lindner, Fluctuation-dissipation relations for spiking neurons, *Phys. Rev. Lett.* **129**, 198101 (2022).
- [12] D. G. Clark, L. F. Abbott, and A. Litwin-Kumar, Dimension of activity in random neural networks, *Phys. Rev. Lett.* **131**, 118401 (2023).
- [13] F. Puttkammer and B. Lindner, Fluctuation-response relations for integrate-and-fire models with an absolute refractory period, *Biol. Cybern.* 10.1007/s00422-023-00982-9 (2024).
- [14] R. F. Fox, Functional-calculus approach to stochastic differential equations, *Phys. Rev. A* **33**, 467 (1986).
- [15] P. Hänggi and P. Jung, Colored noise in dynamical systems, *Adv. Chem. Phys.* **89**, 239 (1994).
- [16] U. M. B. Marconi, A. Puglisi, L. Rondoni, and A. Vulpiani, Fluctuation-dissipation: Response theory in statistical physics, *Phys. Rep.* **111**, 461 (2008).
- [17] G. A. Athanassoulis and K. I. Mamis, Extensions of the Novikov-Furutsu theorem, obtained by using Volterra functional calculus, *Phys. Scripta* **94**, 115217 (2019).
- [18] T. W. Margrie, M. Brecht, and B. Sakmann, In vivo, low-resistance, whole-cell recordings from neurons in the anaesthetized and awake mammalian brain, *Pflug. Arch. Eur. J. Phys.* **444**, 491 (2002).
- [19] J. Dose, G. Doron, M. Brecht, and B. Lindner, Noisy juxtacellular stimulation in vivo leads to reliable spiking and reveals high-frequency coding in single neurons, *J. Neurosci.* **36**, 11120 (2016).
- [20] T. Tchumatchenko, A. Malyshev, F. Wolf, and M. Volgushev, Ultrafast population encoding by cortical neurons, *J. Neurosci.* **31**, 12171 (2011).
- [21] H. Köndgen, C. Geisler, S. Fusi, X.-J. Wang, H.-R. Luescher, and M. Giugliano, The dynamical response properties of neocortical neurons to temporally modulated noisy inputs in vitro, *Cereb. Cortex* **18**, 2086 (2008).
- [22] W. Bialek, F. Rieke, R. de Ruyter van Steveninck, and D. Warland, Reading a neural code, *Science* **252**, 1854 (1991).
- [23] B. W. Knight, Relationship Between Firing Rate of a Single Neuron and Level of Activity in a Population of Neurons - Experimental Evidence for Resonant Enhancement in Population Response, *J. Gen. Physiol.* **59**, 767 (1972).
- [24] H. Markram, J. Lübke, M. Frotscher, A. Roth, and B. Sakmann, Physiology and anatomy of synaptic connections between thick tufted pyramidal neurones in the developing rat neocortex., *J. Physiol.* **500**, 409 (1997).
- [25] L. Badel, S. Lefort, R. Brette, C. C. H. Petersen, W. Gerstner, and M. J. E. Richardson, Dynamic i-v curves are reliable predictors of naturalistic pyramidal-neuron voltage traces, *J. Neurophysiol.* **99**, 656 (2008), pMID: 18057107.

- [26] M. J. E. Richardson and R. Swarbrick, Firing-rate response of a neuron receiving excitatory and inhibitory synaptic shot noise, *Phys. Rev. Lett.* **105**, 178102 (2010).
- [27] G. Last and M. Penrose, *Lectures on the Poisson Process*, Institute of Mathematical Statistics Textbooks (Cambridge University Press, 2017).
- [28] V. Volterra, *Theory of Functionals and of Integral and Integro-differential Equations*, Dover Books on Intermediate and Advanced Mathematics (Dover Publications, 1959).
- [29] R. L. Stratonovich, *Topics in the Theory of Random Noise* (Gordon and Breach, New York, 1967).
- [30] M. S. Bartlett, The spectral analysis of point processes, *J. R. Stat. Soc. B Met.* **25**, 264 (1963).
- [31] J. Turner, *Atoms, Radiation, and Radiation Protection* (Wiley, 2008).
- [32] C. M. Natarajan, M. G. Tanner, and R. H. Hadfield, Superconducting nanowire single-photon detectors: physics and applications, *Superconductor Science and Technology* **25**, 063001 (2012).
- [33] H. G. Stever, The discharge mechanism of fast g-m counters from the deadtime experiment, *Phys. Rev.* **61**, 38 (1942).
- [34] R. Valivarthi, I. Lucio-Martinez, A. Rubenok, P. Chan, F. Marsili, V. B. Verma, M. D. Shaw, J. A. Stern, J. A. Slater, D. Oblak, S. W. Nam, and W. Tittel, Efficient bell state analyzer for time-bin qubits with fast-recovery wsi superconducting single photon detectors, *Opt. Express* **22**, 24497 (2014).
- [35] L. Mandel and E. Wolf, *Optical Coherence and Quantum Optics*, EBL-Schweitzer (Cambridge University Press, 1995).
- [36] R. Brette and W. Gerstner, Adaptive exponential integrate-and-fire model as an effective description of neuronal activity, *J. Neurophysiol.* **94**, 3637 (2005), PMID: 16014787.
- [37] L. Badel, S. Lefort, T. K. Berger, C. C. H. Petersen, W. Gerstner, and M. J. E. Richardson, Extracting nonlinear integrate-and-fire models from experimental data using dynamic $i-v$ curves, *Biol. Cybern.* **99**, 361 (2008).
- [38] R. Jolivet, F. Schürmann, T. K. Berger, R. Naud, W. Gerstner, and A. Roth, The quantitative single-neuron modeling competition, *Biol. Cybern.* **99**, 417 (2008).
- [39] C. Teeter, R. Iyer, V. Menon, N. Gouwens, D. Feng, J. Berg, A. Szafer, N. Cain, H. Zeng, M. Hawrylycz, C. Koch, and S. Mihalas, Generalized leaky integrate-and-fire models classify multiple neuron types, *Nat. Commun.* **9**, 709 (2018).
- [40] L. F. Abbott and C. van Vreeswijk, Asynchronous states in a network of pulse-coupled oscillators, *Phys. Rev. E.* **48**, 1483 (1993).
- [41] N. Brunel, Dynamics of sparsely connected networks of excitatory and inhibitory spiking neurons, *J. Comput. Neurosci.* **8**, 183 (2000).
- [42] J. Schuecker, M. Diesmann, and M. Helias, Modulated escape from a metastable state driven by colored noise, *Phys. Rev. E* **92**, 052119 (2015).
- [43] S. Ostojic, Two types of asynchronous activity in networks of excitatory and inhibitory spiking neurons, *Nat. Neurosci.* **17**, 594 (2014).
- [44] S. Wieland, D. Bernardi, T. Schwalger, and B. Lindner, Slow fluctuations in recurrent networks of spiking neurons, *Phys. Rev. E* **92**, 040901(R) (2015).
- [45] G. K. Ocker, Republished: Dynamics of stochastic integrate-and-fire networks, *Phys. Rev. X* **13**, 041047 (2023).
- [46] M. Layer, M. Helias, and D. Dahmen, Effect of synaptic heterogeneity on neuronal coordination, *PRX Life* **2**, 013013 (2024).
- [47] A. C. Holden, *Models of the Stochastic Activity of Neurons* (Springer-Verlag, Berlin, 1976).
- [48] H. C. Tuckwell, *Stochastic processes in the neurosciences* (SIAM, 1989).
- [49] H. C. Tuckwell and J. B. Walsh, Random currents through nerve membranes. i. uniform poisson or white noise current in one-dimensional cables, *Biol. Cybern.* **49**, 99 (1983).
- [50] C. Koch, *Biophysics of Computation - Information Processing in Single Neurons* (Oxford University Press, New York, Oxford, 1999).
- [51] A. Manwani and C. Koch, Detecting and Estimating Signals in Noisy Cable Structures, I: Neuronal Noise Sources, *Neural Comput.* **11**, 1797 (1999).
- [52] D. Snyder and M. Miller, *Random Point Processes in Time and Space*, Springer Texts in Electrical Engineering (Springer New York, 1991).
- [53] M. Schlungbaum and B. Lindner, Detecting a periodic signal by a population of spiking neurons in the weakly nonlinear response regime, *Eur. Phys. J. E* **46**, 108 (2023).
- [54] J. Henninger, R. Krahe, F. Kirschbaum, J. Grewe, and J. Benda, Statistics of natural communication signals observed in the wild identify important yet neglected stimulus regimes in weakly electric fish, *J. Neurosci.* **38**, 5456 (2018).
- [55] G. K. Ocker, K. Josić, E. Shea-Brown, and M. A. Buice, Linking structure and activity in nonlinear spiking networks, *PLoS Comput. Biol.* **13**, 1 (2017).
- [56] S. Voronenko and B. Lindner, Weakly nonlinear response of noisy neurons, *New J. Phys.* **19**, 033038 (2017).
- [57] R. F. Fox and Y. N. Lu, Emergent collective behavior in large numbers of globally coupled independently stochastic ion channels, *Phys. Rev. E.* **49**, 3421 (1994).
- [58] V. Pernice, B. Staude, S. Cardanobile, and S. Rotter, How structure determines correlations in neuronal networks, *PLoS Comput. Biol.* **7**, 1 (2011).
- [59] S. Jovanović and S. Rotter, Interplay between graph topology and correlations of third order in spiking neuronal networks, *PLoS Comput. Biol.* **12**, 1 (2016).
- [60] R. Brette and W. Gerstner, Adaptive exponential integrate-and-fire model as an effective description of neuronal activity, *J. Neurophysiol.* **94**, 3637 (2005).
- [61] E. M. Izhikevich, Simple model of spiking neurons, *IEEE T. Neural Networks* **14**, 1569 (2003).
- [62] L. Shiau, T. Schwalger, and B. Lindner, Interspike interval correlation in a stochastic exponential integrate-and-fire model with subthreshold and spike-triggered adaptation, *J. Comput. Neurosci.* **38**, 589 (2015).
- [63] L. Ramlow and B. Lindner, Interspike interval correlations in neuron models with adaptation and correlated noise, *PLoS Comput. Biol.* **17**, e1009261 (2021).
- [64] L. F. Abbott and W. G. Regehr, Synaptic computation, *Nature* **431**, 796 (2004).
- [65] J. E. Lisman, Bursts as a unit of neural information: making unreliable synapses reliable, *Trends Neurosci.* **20**, 38 (1997).
- [66] G. Mongillo, O. Barak, and M. Tsodyks, Synaptic theory

- of working memory, *Science* **319**, 1543 (2008).
- [67] B. Lindner, D. Gangloff, A. Longtin, and J. E. Lewis, Broadband coding with dynamic synapses, *J. Neurosci.* **29**, 2076 (2009).
- [68] R. Rosenbaum, J. Rubin, and B. Doiron, Short term synaptic depression imposes a frequency dependent filter on synaptic information transfer, *PLoS Comput. Biol.* **8**, e1002557 (2012).
- [69] M. J. E. Richardson and W. Gerstner, Synaptic shot noise and conductance fluctuations affect the membrane voltage with equal significance, *Neural Comput.* **17**, 923 (2005).
- [70] M. J. E. Richardson and W. Gerstner, Statistics of subthreshold neuronal voltage fluctuations due to conductance-based synaptic shot noise, *Chaos* **16**, 026106 (2006).
- [71] L. Wolff and B. Lindner, A method to calculate the moments of the membrane voltage in a model neuron driven by multiplicative filtered shot noise, *Phys. Rev. E* **77**, 041913 (2008).
- [72] B. Lindner and A. Longtin, Comment on "Characterization of Subthreshold Voltage Fluctuations in Neuronal Membranes" by M. Rudolph and A. Destexhe, *Neural Comput.* **18**, 1896 (2006).
- [73] M. J. E. Richardson, Linear and nonlinear integrate-and-fire neurons driven by synaptic shot noise with reversal potentials, *Phys. Rev. E* **109**, 024407 (2024).
- [74] R. P. Gowers, Y. Timofeeva, and M. J. E. Richardson, Low-rate firing limit for neurons with axon, soma and dendrites driven by spatially distributed stochastic synapses, *PLoS Comput. Biol.* **16**, e1007175 (2020).
- [75] R. P. Gowers and M. J. E. Richardson, Upcrossing-rate dynamics for a minimal neuron model receiving spatially distributed synaptic drive, *Phys. Rev. Research* **5**, 023095 (2023).
- [76] B. Dummer, S. Wieland, and B. Lindner, Self-consistent determination of the spike-train power spectrum in a neural network with sparse connectivity, *Frontiers in Computational Neuroscience* **8**, 10.3389/fncom.2014.00104 (2014).
- [77] P. Lánský, On approximations of stein's neuronal model, *Journal of Theoretical Biology* **107**, 631 (1984).
- [78] P. Lánský, Sources of periodical force in noisy integrate-and-fire models of neuronal dynamics, *Phys. Rev. E* **55**, 2040 (1997).
- [79] A. Kruscha and B. Lindner, Partial synchronous output of a neuronal population under weak common noise: analytical approaches to the correlation statistics, *Phys. Rev.* **94**, 022422 (2016).
- [80] W. Schottky, On spontaneous current fluctuations in various electrical conductors, *J. Micro/ Nanolithogr. MEMS MOEMS* **17**, 041001 (2018).